29th Congress of the International Council of the Aeronautical Sciences
St. Petersburg, Russia; September 7-12, 2014

NUMERICAL STUDY OF ICE ACCRETION ON ROTATING AERO-ENGINE CONE

W. Dong, J. J. Zhu, M. Zheng, R. Wang
*** School of Mechanical Engineering, Shanghai Jiao Tong University**

Keywords: *aero engine icing, heat and mass transfer, water film flow, numerical simulation*

Abstract

Numerical simulation of ice accretion on a rotating aero-engine cone under icing condition is presented. The flow field around the rotating cone is obtained by computational fluid dynamic code. The trajectories of supercooled water droplets and the collection efficiency are calculated by Eulerian approach. Heat and mass balance on rotating cone surface is taken into account in icing process simulation. The effects of rotating speeds and free stream temperature on the icing process are also studied. The simulation results show that the runback water plays a very important role in icing process and the rotating speed has slightly effect on ice accretion on the cone surface. The effect of different free stream temperature on ice accumulation on the cone surface is also analyzed.

1 Introduction

Ice accretion on the inlet of an aero-engine could adversely affect the characteristics of the inlet flow field and degrade the engine's performance. If the shed ice is sucked into the engine, it may be lead to serious mechanical damages. In order to reduce the hazards caused by in-flight icing, an anti-icing or de-icing system should be used. Hot air bleeding from high pressure compressor is widely used in inlet anti-icing systems. The air for hot-air anti-icing system must be bled from compressor. Air bleeding will lead to engine performance penalties. The de-icing method removes the accumulated ice using electric or hot air to increase the surface temperature to be near or above the freezing point. In some rotating parts of an aero-engine such as rotating cone, ice is removed from surface by centrifugal and aerodynamic force that is larger than ice adhesive force on the surface when ice accumulates to a certain thickness [1]. This method has no great effect on the aero-engine performance. The rotating cone of commercial turbofan engine usually adopts special cone angle design or surface coating to remove ice from surface. It is necessary to investigate the ice accretion on rotating cone surface to predict the ice shedding and inlet aerodynamic characteristics.

The physical processes of ice accretion are complex and are not understood completely. Though significant efforts have been devoted to the research of icing physics, the computational model of icing accretion still requires further development. In recent years, many computational methods of the icing problem are developed to improve the simulation of icing and de-icing process. Computational codes of icing have been developed at NASA (ANTICE [2], LEWICE [3]), McGill University [4], et al. These icing simulation codes usually consist of four basic steps to analyze icing process [5]: computation of flow field around components; determination of super-cooled water droplet trajectories and local collection efficiency; thermal balance analysis of the air-water-ice-body system; computation of the ice shape on the components surface.

Flow field around the body can be obtained by solving Euler or Navier-Stokes equations and the convective heat transfer coefficient on the icing surface can be obtained at the same time. Supercooled water droplet trajectories can be tracked by using the Lagrangian approach or Eulerian approach and subsequently the local

collection efficiency on the surface can be calculated. Hamed et al. [6] presented a methodology for three dimensional numerical simulations of supercooled water droplet trajectories through rotating blades of an aero-engine and gave the results of droplet trajectories, rotor blade impingement locations, and the corresponding water collection efficiency for a transonic fan rotor. Bourgault et al. [7] developed a code using an Eulerian approach to calculate water impact loads on complex geometries. A number of codes of predicting the impingement characteristics of aircraft components have been developed and all give satisfactory results using either Lagrangian or Eulerian approach. A significant effort has been conducted to predict the impingement characteristics of the supercooled large droplet (SLD) in recent years [8, 9].

Most ice accretion codes compute the surface temperature and predict the ice growth rate using heat and mass balance model given by Messinger [10]. The heat balance model is important for predicting ice accretion process and affects the result of the ice shape. Wright et al. [11,12] developed an algorithm to model the two-dimensional transient heat transfer, ice accretion, ice shedding and ice trajectory which arise from the use of an electrothermal pad and examined different numerical methods for solving the transient heat transfer in a deicing system occurring in a multilayered body covered with ice. Al-Khalil [13,14] utilizes the breakup of a uniformly thin liquid film into individual streams or rivulets to more accurately describe the physics of runback water. Yi [15] modified the icing model and used it for numerical simulation of rime, glaze and mixed ice accretion on the airfoil surface. Silva et al. [16] developed a thermal model considering coupled and mass transfer effects for anti-icing numerical simulation. Croce [17] computed the temperature on the icing surface by solving 3D Navier-Stokes equations and solid conduction equation. Dong et al. [18,19] computed and analyzed the performance of an inlet aero-engine strut anti-icing system using conjugated algorithm. Papadakis et al. [20] computed inlet leading edge ice shapes with the LEWICE3D ice accretion code and LEWICE3D ice shapes were found to be in good agreement with experimental results, in terms of ice shape size, horn features, and icing limits. Iuliano et al. [21] developed a approach to simulate the SLD icing phenomena.

Although many efforts have been made on ice shape simulation, few of them focus on the icing process of rotating cones. In this paper, icing processes on rotating cone are studied by numerical simulation. The flow field is solved by 2D axisymmetric Ansys Fluent solver [22]. Droplet collection efficiency is computed by Eulerian approach and ice shape is obtained by adding ice frozen thickness to dynamic control volume. The effects of runback water, rotating speed and free stream temperature on ice shape are discussed.

2 Numerical Methods

2.1 Computation of the Air Flow

Flow field is needed for calculating the droplet impingement property and thermal analysis of the rotating cone. The N-S equations of steady flow in 2D axisymmetric coordinate are solved to obtain the flow field around the cone by using ANSYS FLUENT.

The pressure velocity coupling algorithm is used to generate solutions for the air flow field. The second-order upwind advection scheme is employed for momentum and energy equations. The SST turbulence model is used to close the equations for the flow and heat transfer computation. The boundary layer meshes are refined y+ to less than 1 near the wall surface of the cone.

2.2 Description of Droplet Phase Motion

In most cases, the effects of water droplets on the air flow can be neglected due to the low liquid water content (LWC). The motion of water droplets in air flow field is subject to fluid drag, buoyancy and gravity forces acting on the water droplets. As the supercooled water droplet diameter is usually very small, the effects of buoyancy and gravity forces is small compared with the aerodynamic forces and can be ignored.

Droplets' movement is computed by Eulerian approach. The governing equations of the water droplet phase are described as follows,

$$\frac{\partial \alpha \rho_d}{\partial t} + \nabla \cdot (\alpha \rho_d \vec{v}_d) = 0 \quad (1)$$

$$\frac{\partial \alpha \vec{v}_d \rho_d}{\partial t} + \nabla \cdot (\alpha \rho_d \vec{v}_d \vec{v}_d) = \vec{D} \quad (2)$$

where ρ_d , $\vec{v}_d$ and α are density, velocity and volume fraction of droplet, respectively. $\vec{D}$ is the aerodynamic drag force on water droplet phase. Aerodynamic drag force can be calculated as follows,

$$\vec{D} = C_D \cdot \frac{1}{2} \rho_a |\vec{v}_a - \vec{v}_d| (\vec{v}_a - \vec{v}_d) A_d \quad (3)$$

where A is frontal area of the droplet and equal to $\frac{1}{4}\pi d_d^2$. d_d is diameter of the droplet. C_D is the drag coefficient, which can be obtained by[23],

$$C_D = \frac{24}{\mathrm{Re}_{rel}}(1 + 0.197\,\mathrm{Re}_{rel}^{0.63} + 2.6\times10^{-4}\,\mathrm{Re}_{rel}^{1.38}) \quad (4)$$

and relative Reynolds is defined as,

$$\mathrm{Re}_{rel} = \frac{2\rho_a r_d (\vec{v}_a - \vec{v}_d)}{\mu_a} \quad (5)$$

where subscript a means air phase. Hence, Eqn. (2) can be derived to,

$$\frac{\partial \alpha \vec{v}_d \rho_d}{\partial t} + \nabla \cdot (\alpha \rho_d \vec{v}_d \vec{v}_d) = \frac{3}{4} \frac{C_D \rho_a}{d_d \rho_d} |\vec{v}_a - \vec{v}_d| (\vec{v}_a - \vec{v}_d) \quad (6)$$

Droplet collection efficiency β can be obtained as,

$$\beta = \frac{\alpha}{\alpha_\infty} \frac{\vec{v}_d \cdot \vec{n}}{|\vec{v}_{d,\infty}|} \quad (7)$$

where subscript ∞ refers to the value of free stream and $\vec{n}$ is the unit normal vector on the rotating cone surface.

2.3 Model of Heat and Mass Balance

The impinging water will run back on the cone surface due to aerodynamic force if the impinged water cannot be frozen completely. This model of runback water is shown in Fig. 1.

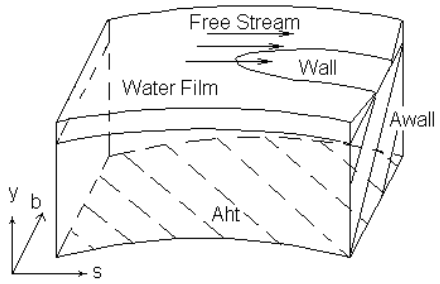

Fig. 1 Water Film Flow on cone Surface

The mass balance equation of run back flow is,

$$\dot{m}_{in} + \dot{m}_{imp} = \dot{m}_{out} + \dot{m}_{evap} + \dot{m}_{ice} \quad (8)$$

where $\dot{m}_{in}$, $\dot{m}_{imp}$, $\dot{m}_{out}$, $\dot{m}_{evap}$ and $\dot{m}_{ice}$ represent the mass flow rate of incoming water, water droplets that impinged on surfaces, outflow water, evaporated water and frozen water on each surface control volume, respectively.

The mass flow rate of impinged water droplets is related to the droplet collection efficiency,

$$\dot{m}_{imp} = v_a \beta A_{ht} LWC \quad (9)$$

where A_{ht} is the surface area of the control volume, and LWC is the liquid water content.

The mass flow rate of evaporated water on the cone surface can be calculated as,

$$\dot{m}_{evap} = FA_{ht} \frac{0.622 I_{water-vapor} h_{air}}{c_{p,water}} \left(\frac{p_{v,surface} - p_{v,e}}{p_e - p_{v,surface}}\right) \quad (10)$$

where $p_{v,surface}$ and $p_{v,e}$ refers to the saturated vapor pressure at the cone surface temperature and the temperature of air flow boundary layer respectively. p_e is the local pressure of air flow. $I_{water-vapor}$ is the latent heat of evaporation. h_{air} is the convective heat transfer coefficient of air flow on the cone surface. $c_{p,water}$ is specific heat of water.

Under icing conditions, the energy balance equation is as follows,

$$\dot{m}_{imp}(\frac{\vec{v}_{d,\infty}^{\,2}}{2}+c_{p,water}T_{\infty})+\dot{m}_{ice}I_{water-ice}+\dot{m}_{in}c_{p,water}T_{in}$$
$$=\dot{m}_{out}c_{p,water}T_{out}+\dot{m}_{evap}I_{water-vapor}+q_{conv}A_{ht} \quad (11)$$

where $I_{water-ice}$ is the latent heat of condensation, q_{conv} is the heat transfer flux due to convection, T_{in} and T_{out} are temperatures of the water flowing into the control volume from upstream and the water running back to the next control volume , respectively.

Mass and energy balance equations are solved from the stagnation point of the cone and are marched downstream in each control volume along the cone surface. Then $\dot{m}_{ice}$ can be obtained in each surface control volume. The accreted ice height in each surface control volume can be calculated as,

$$h_{ice}=\frac{\dot{m}_{ice}}{\rho_{ice}A_{ht}} \quad (12)$$

During the icing process simulation, ice is assumed to accrete at the normal direction of the cone surface

3 Results and Discussions

3.1 Case Conditions

A typical rotating cone configuration is chosen to simulate the icing process and discuss the effects of runback water, rotating speed and free stream temperature on ice shape on the cone surface. The cone configuration is shown in Fig.2.

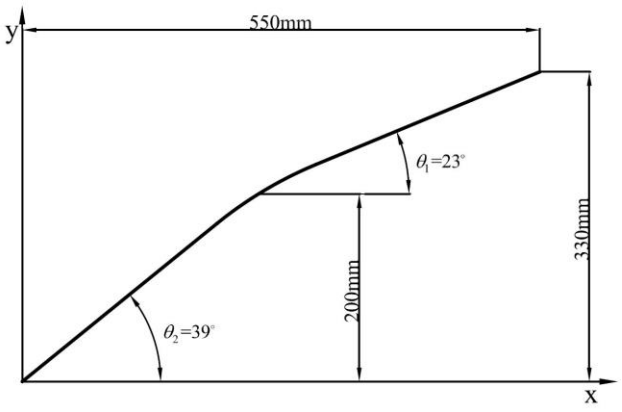

Fig. 2 The computational cone configuration

Airflow around the cone is solved under 2D axisymmetric coordinate by Ansys Fluent. Rotating is simulated by using the moving wall boundary. The air velocity of free stream in all simulations is 40m/s in axial direction. Medium volume diameter (MVD) of water droplets is 20μm and liquid water content (LWC) is 2g/m^3 in all simulations. Transient method is used to simulate the icing process.

The computation cases at different rotating speeds of 0, 3000 and 6000rpm are simulated to analyze the rotating effect with the free stream temperature of -10℃ for three cases. To find out the effect of free stream temperature on icing shape on the cone, three other cases at different free stream temperature of -5, -10, -20℃ are also studied at the rotating speed of 3000rpm.

3.2 Effects of Runback Water Flow

Fig. 3 shows the simulated ice shapes on the cone surface under icing condition of free stream temperature of -10℃, free stream velocity of 40m/s, MVD of 20μm, LWC of 2g/m^3 and rotating speed of 3000rpm for ice accretion time of 3 minutes. It is assumed that the impinged water is frozen immediately after impingement, the maximum ice thickness on the leading edge of the cone will be about 6mm. The simulated ice thickness decreases to about 2mm when the runback water model on the cone surface is considered. The size of ice thickness is relatively small compared with the cone size. In glaze icing condition, impinged water on the leading region cannot be frozen completely and will run back along the cone surface. In the rear region of the cone, the thickness of ice layer is about 0.2mm at the axial location of 232mm, which is very thin due to no water droplets impinging there.

Local collection efficiency of impinged water droplets before icing and 3 minutes after icing is shown in Fig. 4. After ice accretes on the cone surface, the maximum collection efficiency and impingement region become larger than those with no ice on the cone surface. It can be deduced that icing accumulation rate can be larger as icing time goes.

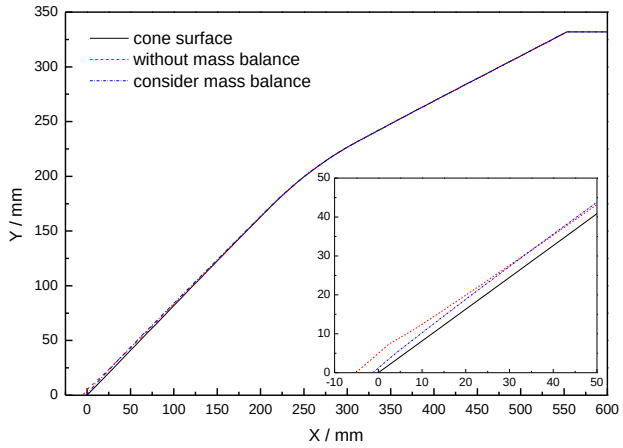

(a)

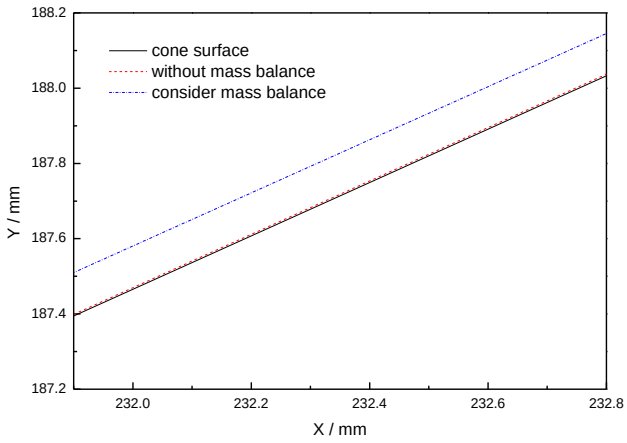

(b)

Fig. 3 Simulated ice shapes for ice accretion time of 3 minutes at free stream temperature of -10℃ and rotating speed of 3000rpm

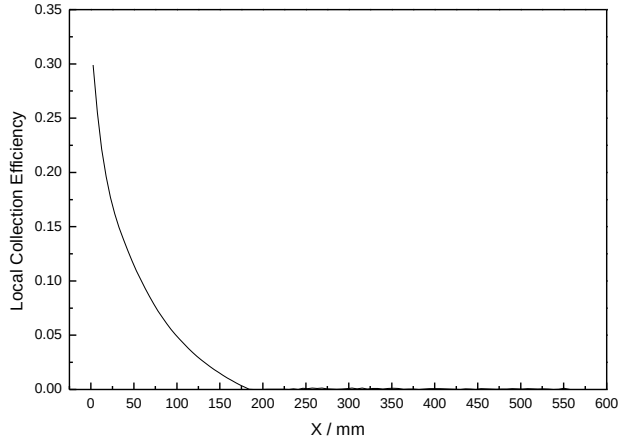

(a) no ice on the cone surface

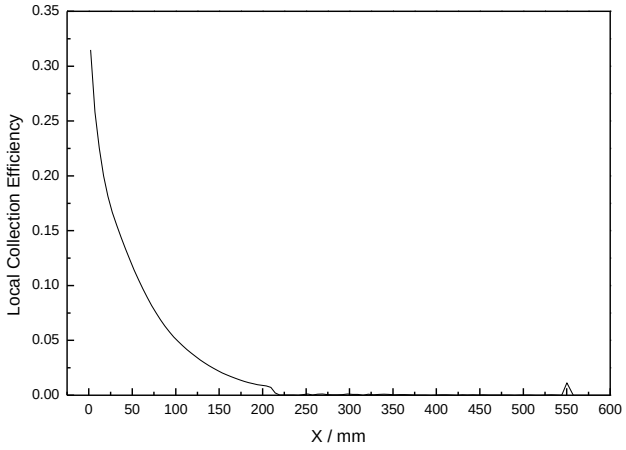

(b) 3 minutes icing shape on the cone

Fig. 4 Local collection efficiency at rotating speed of 3000rpm

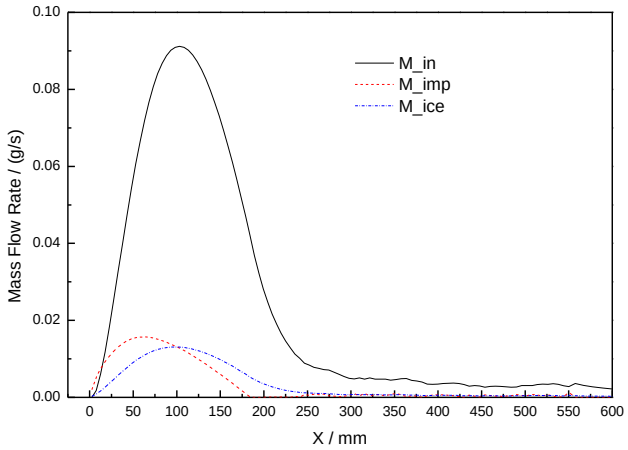

(a) before icing

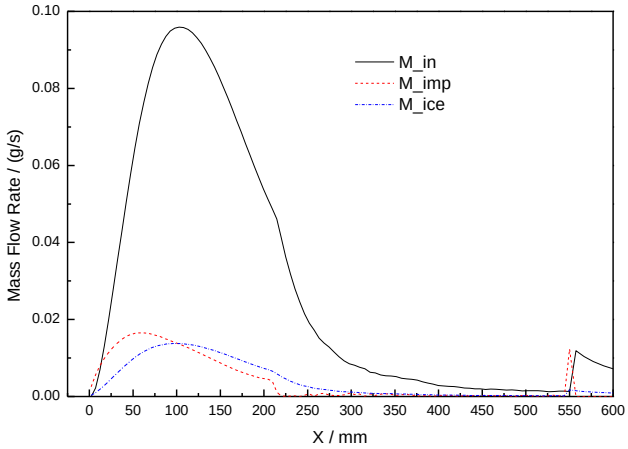

(b) 3 minutes after Icing

Fig. 5. Water mass flow rate on the surface at free stream velocity of -10℃ and rotating speed of 3000rpm

The mass rate distributions of runback water, impingement water and icing water on the cone surface are shown in Fig. 5. It can be found that the mass rate of runback water is larger than the mass rate of impingement water under this icing condition. The runback water will have more effects on the ice shape on the cone surface under glaze icing conditions. As impingement region and collection efficiency become larger after ice accreting on the cone surface, mass rates of both runback water and impingement water also become larger.

3.3 Effects of rotating speeds

Fig. 6 shows the local collection efficiency distribution on the cone surface without ice at different rotating speeds. The computational results show that the rotating speed has effects on the maximum value and distribution of local collection efficiency, but the effects are small. For stationary cone, more water droplets impinge on the cone surface at the regions of x=125mm to x=225mm and the rear region. The characteristics of local collection efficiency distribution at different rotating speed are different due to the effect of air tangential velocity near the cone. The air flow tangential velocity becomes larger as the radius of cone increases. The larger air tangential velocity makes water droplets more difficult to keep their moving direction and leads to the decrease of water droplets impingement.

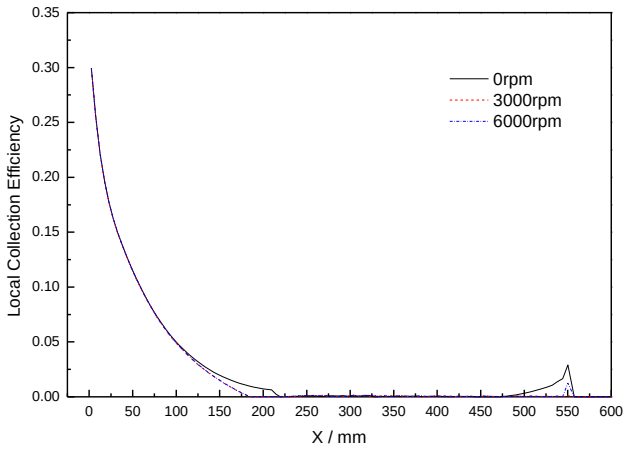

Fig. 6 Local collection efficiency distribution at different rotating speed

Simulated ice shapes at different rotating speeds of the cone are shown in Fig. 7. At the leading edge of the cone, three ice shapes are similar. At the rear region of the cone, ice thickness on the stationary cone is larger than the thickness of rotating cone due to larger collection efficiency. The ice shapes on the whole cone are similar at rotating speeds of 3000rpm and 6000 rpm, the ice thickness at 3000rpm is slightly larger than that at 6000rpm.

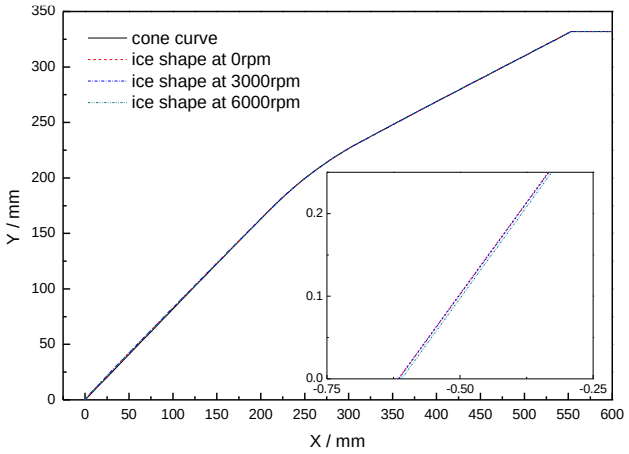

(a)

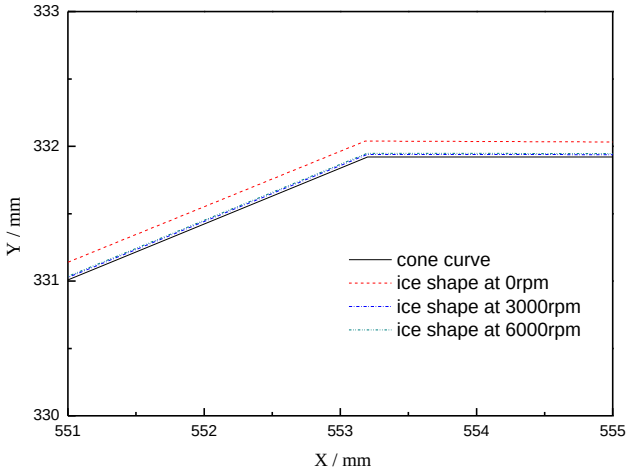

(b)

Fig. 7 Simulated ice shapes for ice accretion time of 3 minutes at different rotating speed

3.4 Effects of free stream temperature

The local collection efficiency on the cone surface is the same for different temperatures of free stream due to the same free stream velocity. The cone rotating speed is 3000rpm. However, as icing process goes, different free stream

temperatures may lead to different ice shapes, which can affect air velocity in the flow field as well as the droplet collection efficiency.

Fig. 8 shows the simulated ice shapes for ice accretion time of 3 minutes under different free stream temperatures. At the leading edge of the cone, higher free stream temperature leads to thinner ice. Much water is frozen at the leading edge and the mass flow rate of runback water is small, thus ice at lower temperature is thinner than that at higher temperature on the rear surface of the cone.

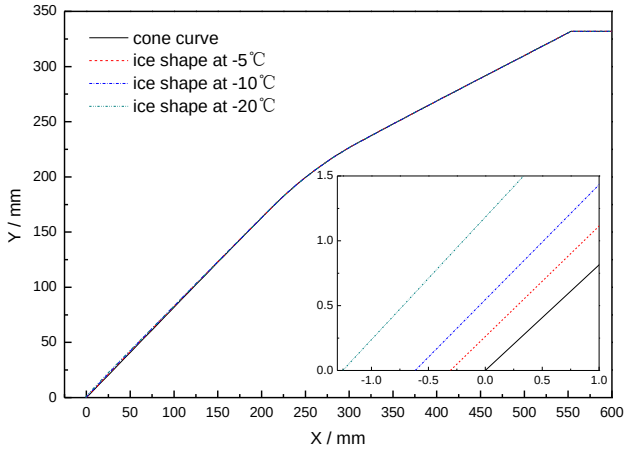

(a)

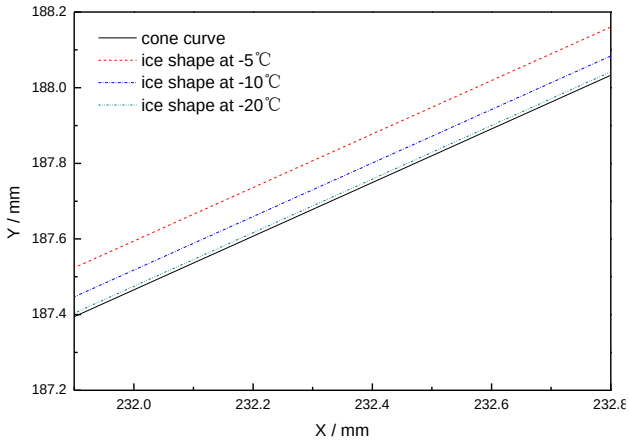

(b)

Fig. 8 Simulated ice shapes for ice accretion time of 3 minutes at different free stream temperatures

4 Conclusions

A numerical simulation method of rotating cone icing process with considering the mass and energy balance is presented and applied to study the icing process of a typical rotating aero-engine cone. The flow field around the rotating cone is computed by CFD code. The trajectories of supercooled water droplets and the collection efficiency are calculated by Eulerian approach. The main conclusions of this paper are as follows

- Water mass balance is recommended to be taken into account in the icing simulation because runback water plays a very important role in icing process;
- As ice accretes, droplet collection efficiency becomes larger in both maximum value and impingement region for rotating cone.
- Rotating speed affects ice shape slightly. At the rear region of the cone, ice thickness on the stationary cone is larger than the thickness of rotating cone due to larger collection efficiency.
- Much water is frozen at the leading edge and the mass flow rate of runback water is small for lower free stream temperature. The ice will be thicker for lower free stream temperature at the leading edge of the cone, but thinner than that of higher free stream temperature on the rear surface of the cone.

References

[1] Dong W, Ding J and Zhou Zh. Experimental Study on the Ice Freezing Adhesive Characteristics of Metal Surfaces. *Journal of Aircraft*, Vol.51, No.3, pp.719–726, 2014.

[2] AI-Khalil K, Miller D and Wright W. Validation of NASA Thermal Ice Protection Computer Codes.III – The validation of ANTICE. AIAA Paper 97-0051, 1997.

[3] Wright W. LEWICE 2.2 Capabilities and Thermal Validation. AIAA Paper 2002-0383, 2002.

[4] Nakakita K, Nadarajah S and Habashi W. Toward Real-Time Aero-Icing Simulation of Complete Aircraft via FENSAP-ICE. *Journal of Aircraft*, Vol.47, No.1, pp.96–109, 2010.

[5] Kind R J, Potapczuk M G, Feo A, Golia C and Shah A D. Experimental and Computational Simulation of In-flight Icing Phenomena. *Progress in Aerospace Science*, Vol.34, No.5-6, pp. 257-345, 1998.

[6] Hamed A, Das K and Basu D. Numerical simulations of ice droplet trajectories and collection efficiency on

aero-engine rotating machinery. AIAA Paper 2005-1248, 2005.

[7] Bourgault Y, Boutanios Z and Habashi W G. Three-Dimensional Eulerian Approach to Droplet Impingement Simulation Using FENSAP-ICE,Part 1: Model, Algorithm, and Validation. *Journal of Aircraft*, Vol.37, No.1, 2000, pp.95–103.

[8] Wright W B, Potapczuk M G and Levinson L H. Comparison of LEWICE and GlennICE in the SLD Regime. AIAA Paper 2008-439, 2008.

[9] Villedieu Ph, Trontin P, Guffond D and Bobo D. SLD Lagrangian modeling and capability assessment in the frame of ONERA 3D icing suite. AIAA Paper 2012-3132, 2012.

[10] Messinger B L. Equilibrium Temperature of an Unheated Icing Surface as a Function of Air Speed. *Journal of the Aeronautical Sciences*, Vol.20, No.1, pp.29–42.1953.

[11] Wright WB, Keith T G and De Witt K J. Transient Two dimensional Heat Transfer Through a Composite Body with Application to Deicing of Aircraft Components. AIAA Paper 1988-0358,1988.

[12] Wright W B, Keith T G and De Witt K J. Numerical Simulation of Icing, Deicing, and Shedding. AIAA Paper 1991-0665, 1991.

[13] Al-Khalil K M. Numerical Simulation of an Aircraft Anti-icing System Incorporating a Rivulet Model for the Runback Water. Ph.D. Dissertation, Univ. of Toledo, Toledo, OH, 1991.

[14] Al-Khalil K M, Keith T G, DeWitt K J, Nathman J K and Dietrich D A. Thermal Analysis of Engine Anti-icing Systems. *Journal of Propulsion and Power*. Vol.6, No.5, pp.628-634, 1990.

[15] Yi X. Numerical Computation of Aircraft Icing and Study on Icing Test Scaling Law. Ph.D. Dissertation, China Aerodynamics Research and Development Center, Mianyang, 2007.

[16] Silva G A L, Mattos Silvares O and Jesus Zerbini E J G. Numerical Simulation of Airfoil Thermal Anti-Ice Operation Part 1: Mathematical Modeling. *Journal of Aircraft.* Vol.44, No.2, pp.627-633, 2007.

[17] Croce G, Beaugendre H and Habashi W G. CHT3D: FENSAPICE Conjugate Heat Transfer Computations with Droplet Impingement and Runback Effects. AIAA Paper 2002-0386, 2002.

[18] Dong W, Zhu J and Zhao Q Y. Numerical Simulation Analysis of a Guide Vane Hot Air Anti-icing System. AIAA Paper 2011-3944, 2011.

[19] Dong W, Zhu J, Zhou Zh and Chi X. Heat Transfer and Temperature Analysis of an Anti-icing System for an Aero-engine Strut under Icing Condition. AIAA Paper 2012-2753, 2012.

[20] Michael Papadakis M, Yeong H W, Wong S C and Wong S H. Comparison of Experimental and Computational Ice Shapes for an Engine Inlet. AIAA Paper 2010-7671, 2010.

[21] Iuliano E, Mingione G and Petrosino F. Eulerian Modeling of Large Droplet Physics Toward Realistic Aircraft Icing Simulation. *Journal of Aircraft*, Vol.48, No.5, pp.1621–1632, 2011.

[22] ANSYS INC. Ansys Fluent User's Guide Release 14.5, 2012.

[23] Clift R, Grace J and Weber M. Bubbles, drops and particles, 1978.

Acknowledgement

Support given by the National Natural Science Foundation of China under Grant Nos. 51076103 and 11272212.

Contact Author Email Address

mailto:wdong@sjtu.edu.cn

Copyright Statement